Contract No.:

This manuscript has been authored by Savannah River Nuclear Solutions (SRNS), LLC under Contract No. DE-AC09-08SR22470 with the U.S. Department of Energy (DOE) Office of Environmental Management (EM).

Mechanisms contributing to dark current across metal/CdMnTe/metal structures

V. Sklyarchuk[1], P. Fochuk[1], S. Solodin[1], Z. Zakharuk[1], A. Rarenko[1], A. E. Bolotnikov[2] and R. B. James[2,3]

[1]Chernivtsi National University, 2, Kotsiubynskoho Str., Chernivtsi, Ukraine, 58012
[2]Brookhaven National Laboratory, Upton, NY, USA, 11973
[3]Savannah River National Laboratory, Aiken, SC, USA, 29803

ABSTRACT

Studies of the electro-physical properties of n-type semi-insulating indium-doped Cd(Mn)Te crystals with a resistivity ~ (4-5)×10^{10} Ohm×cm at T = 300 K were carried out. Structures with both ohmic (In/Cd(Mn)Te/In) and rectifying (Ni/Cd(Mn)Te/In) contacts were fabricated and tested. It was found that in the case of the Ni/Cd(Mn)Te/In structure, the charge transport can be explained by the generation of currents in the space-charge region and the space-charge limited current (SCLC) at high voltages, while Ohm's law is valid only at the initial section of the volt-ampere (*I-V*) curve. Calculations of the dependence of the generation current on the voltage according to the Sah-Noyce-Shockley model were performed. For the In/Cd(Mn)Te/In structure, we observed the initial part of the *I-V* curve obeys Ohm's law, and the SCLCs with participation of deep centers (traps) in the semi-insulating crystal were observed at greater voltages. The concentration of deep centers (N_t ~ 7.4×10^{10} cm^{-3}) responsible for the trap mechanism in SCLC In/Cd(Mn)Te/In structures was calculated. The energy position E_{t1} of the deep level was determined (calculated from the valence band edge at E_{t1}= 0.89-0.9 eV). We demonstrated that SCLC was the main mechanism limiting the operating voltage and, consequently, a major factor in the performance and use of Cd(Mn)Te-based ionizing radiation detectors with ohmic contacts.

Keywords: Schottky contact, ohmic contact, space-charge limited currents, Cd(Mn)Te crystals.

1. INTRODUCTION

Over the past few decades, the need for semiconductor X- and gamma-ray detectors in science, medicine, industry, forensics, environmental monitoring and other areas has rapidly increased [1]. The basis of such detectors is a semiconductor crystal, in which an electric field is created by an applied bias. Each incident particle generates a specific number of electron-hole pairs per interaction event. In spectrometric detectors, each photon generates an amount of charge that is proportional to the total deposited energy.

CdTe was proposed as a promising material for X/γ-ray detectors in early 1960s [2]. Further developments put CdTe ahead of other semiconductor candidate materials [3-7]. The main advantage of CdTe detectors in comparison to high-purity germanium is the ability to operate without cryogenic cooling and the greater sensitivity to higher X- or gamma-ray energies due to the higher atomic numbers of Cd and Te. CdTe single crystals require high purity and homogeneity for good performance as detectors, which has been difficult to achieve at the current level of technology. It was found in the late 1990s that the crystal quality and electron charge colletion improves with the transition from CdTe to $Cd_{1-x}Zn_xTe$ ($x \approx 0.1$-0.2) solid solution, but other problems remain. The new search for X/γ-ray detector materials continues, and $Cd_{1-x}Mn_xTe$ solid solutions deserve special attention due to their material properties [8-15].

One of the challenges of $Cd_{1-x}Zn_xTe$ technology is related to Zn segregation during growth, which leads to compositional non-uniformity of the grown crystals. $Cd_{1-x}Mn_xTe$ is free from this problem, since the Mn segregation factor in CdTe is close to 1, but not greater than 1, as for Zn. Moreover, to increase the CdTe band-gap to the optimal value required for detectors, one needs to add only half of the manganese to CdTe, compared to the amount of zinc that must be added. The reduction of manganese content, as well as the lack of Mn segregation, has the potential to greatly improve the technology of semi-insulating $Cd_{1-x}Mn_xTe$ by providing more homogeneous material for manufacturing. Semi-insulating semiconductors ($\rho \geq 10^9$ Ohm-cm) are traditionally used for the manufacturing of ionizing radiation detectors. It is believed that the high resistivity of the semiconductors provides an acceptably low dark current and, accordingly, the low noise required for high energy resolution. To prevent recombination (capture) of electrons and

holes, a high electric-field strength is required, and the dark current in the detector should be relatively insignificant, which is achieved by using material with a high resistivity.

In the case of detector fabrication, the contacts are usually metallic, and they are made to the semi-conductor crystal with the desired form [16]. Contacts are needed to apply the voltage to the crystal at the preferred value. At the same time, the impact of the contact type on the current-voltage characteristics (*I-V*) has not yet been fully undeerstood, especially when it concerns to semi-insulating crystals. Usually it is believed that one of the methods of dark current reduction (in addition to increasing the bulk resistivity ρ) is the creation of a p-n junction in the crystal or a Schottky diode. On the other hand, it is noted that this may be accompanied by a decrease in the detector sensitivity at the high-energy quanta region depended on the width and shape of the depletion region.

The purpose of our work is to investigate the influence of the type of contact on the metal-semi-insulating semiconductor *I-V*, particularly the effect of the contact type on the mechanisms of dark current passage in Metal/Cd(Mn)Te/Metal structures. Cd(Mn)Te crystals with a band-gap of E_g = 1.68 eV (x=0.14) and resistivity of (4-5)×10^{10} Ohm-cm at 300 K were used in this study. Cd(Mn)Te crystals were grown by the Bridgman method after synthesis of purified material with a Te zone. We used indium and nickel as the contact materials. Two classical structures were investigated: a structure with two ohmic contacts and a classical diode with one rectifying and one ohmic contact. The structure with two rectifying contacts is also used for the manufacture of ionizing radiation detectors, but from our point of view, the *I-V* analysis of such structures is much more complicated. Very different *I-V curves* may be observed depending on the thickness of the crystal, resistivity, and electron mobility-lifetime ($\mu\tau$) product. The dark current of such structures is controlled by the contact operating in the reverse-bias direction. However, when the currents generated by the space charge (SCR) become significant, caused by the bias in the forward direction of the second rectifying contact, a switching effect may be observed.

2. EXPERIMENTAL RESULTS

Indium-doped $Cd_{1-x}Mn_xTe$ (x=0.14) crystals were grown at the Chernivtsi National University by the Bridgman method after Te-zone purification [17]. The crystals possessed an n-type conductivity with a resistivity ~ (4-5)×10^{10} Ohm-cm at 300 K. From the optical measurements, the band-gap of the crystals was determined to be E_g=1.68 eV.

The fabrication of an Ohmic contact is a rather complicated technological process, especially when the concentration of uncompensated impurities is $N \leq 10^{12}$ cm^{-3}. If $N \leq 10^{12}$ cm^{-3}, then even a slight curvature of the energy bands, when the contact is formed, may lead to the formation of a space-charge region (SCR), in which case the apparent resistance may be greater than the resistance of the neutral part of the crystal. With further voltage increases, the SCR increases, which complicates the *I-V* analysis. Therefore, considerable care is required to fabricate an ohmic contact.

Semiconductor wafers of 5x5x1.5 mm^3 size were fabricated from the Cd(Mn)Te ingot by the method of string cutting and the corresponding mechanical grinding and polishing. After mechanical polishing, the wafers were chemically etched in bromine-methanol solution and then washed in methanol. Immediately before the metal was applied by thermal vacuum evaporation, the semiconductor surface was treated in an argon plasma as described in [18]. To form an ohmic contact, indium was sputtered in a vacuum of less than 10^{-5}-10^{-6} Torr. The contact area of 10 mm^2 was set by a molybdenum mask, and the substrate temperature was 390-410 K. After indium evaporation without reducing the pressure inside the vacuum chamber, the temperature was increased up to 430 K for 10-15 seconds. An Ohmic contact on the opposite surface was made in a similar manner, thus fabricating the In/Cd(Mn)Te/In structure. To create the Ni/Cd(Mn)Te/In structure, nickel was first deposited in a vacuum at a substrate temperature of 400-410 K. Prior to Ni deposition, the surface was treated by an argon plasma, but differently than for a rectifying contact. An Ohmic contact was created on the opposite side of the crystal in the same way as for the In/Cd(Mn)Te/In structure.

The *I-V* curves measured for In/Cd(Mn)Te/In and Ni/Cd(Mn)Te/In structures are shown in Figs. 1 (a, b). The *I-V* curve of the In/Cd(Mn)Te/In structure was found to be symmetric with respect to the voltage polarity. The value of the dark current was proportional to the contact area, as verified by making the contacts with areas of 2 mm^2, 5 mm^2 and 10 mm^2. The structure did not generate the photo-electromotive force (FEMF) when illuminated with an incandescent lamp. For Ni/Cd(Mn)Te/In, the reverse bias current was significantly lower. In addition, the dark current was not proportional to the contact area, but to the contact perimeter. Moreover, when the nickel-contact side was illuminated, the structure generated a FEMF of ~ 0.4-0.5 V. The mechanism of the dark current formation of the In/Cd(Mn)Te/In structure is similar to the case of the forward-biased Ni/Cd(Mn)Te/In structure. Therefore, we confine ourselves to analyze the *I-V* relationship for the In/Cd(Mn)Te/In and analyzing the *I-V* for the Ni/Cd(Mn)Te/In at a reverse-bias condition.

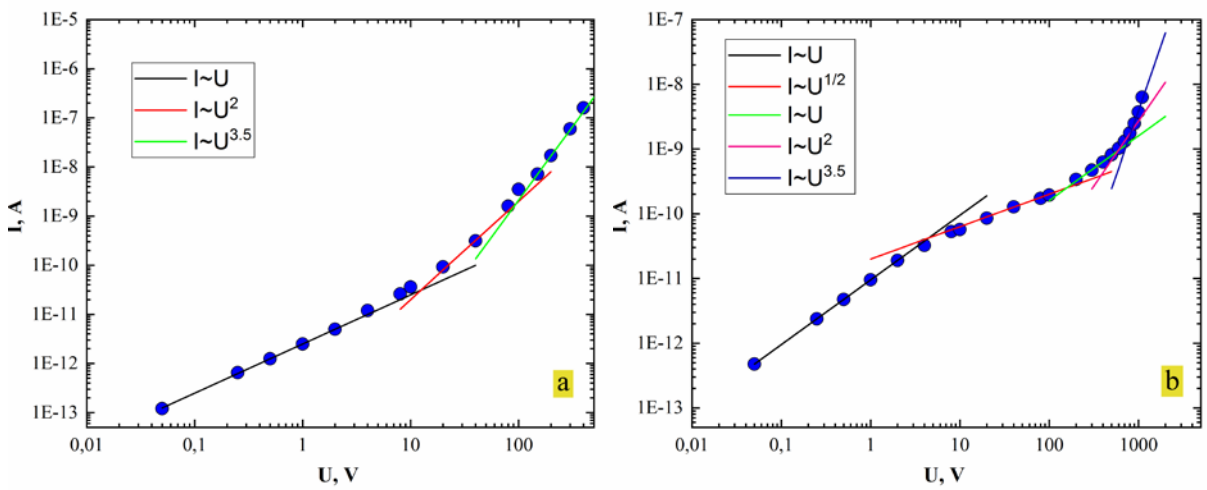

Fig. 1. (a) *I-V* of the In/Cd(Mn)Te/In structure, (b) *I-V* of the Ni/Cd(Mn)Te/In structure at a reverse bias condition (power source "minus" to the nickel electrode). The crystal thickness for both types of structures is 1.5 mm, and the contact area is 10 mm^2. T = 290 K.

As seen in Fig. 1, in general the *I-V* curves of the In/Cd(Mn)Te/In and Ni/Cd(Mn)Te/In structures are substantially different. For the In/Cd(Mn)Te/In structure, we observed three characteristic regions: a linear $I{\sim}U$ in the voltage range ~ (0.05-12) V, a quadratic $I{\sim}U^2$ at (12-110) V and a power dependence $I{\sim}U^{3.5}$ at (110-500) V, while for the Ni/Cd(Mn)Te/In structure, we observed five characteristic areas at different voltage ranges: first a linear $I{\sim}U$ – (0.05-4.5) V, a sublinear $I{\sim}U^{1/2}$ – (5-200) V, a linear $I{\sim}U$ – (200-600) V, a quadratic $I{\sim}U^2$ – (600-850) V, and a power dependence $I{\sim}U^{3.5}$ – (850-1200) V. The voltage range of each characteristic area was determined by the intersection points of the corresponding direct dependences (see Figs. 1 (a, b)). Similarly, for both structures, only the initial linear region of the I-V was found, where Ohm's law was demonstrated. It becomes particularly evident if we plot the dependence of the differential resistance on the voltage (Fig. 2):

$$\rho_{dif}=dU/dI\times S/d, \tag{1}$$

where S is the contact area, and d is the thickness of the crystal.

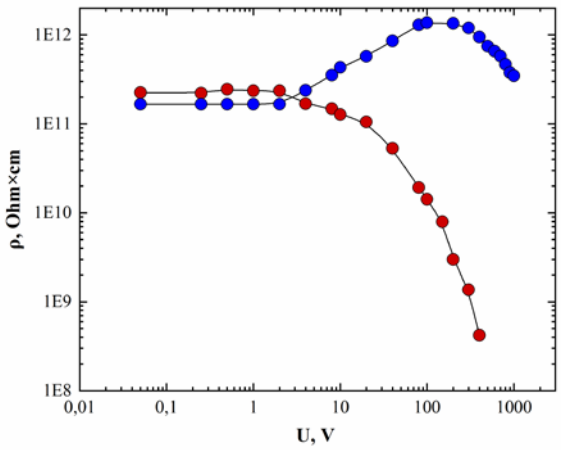

Fig. 2. Dependence of the differential resistance on the voltage: for the In/Cd(Mn)Te/In structure - blue circles and for the Ni/Cd(Mn)Te/In - red circles. T=290 K.

As seen in Fig. 2, the dependence of the differential resistance on the voltage is different for the two types of contacts. In the voltage range of 0.05-5 V, the differential resistance is almost the same for both structures and equal to ~2×10^{11} Ohm-cm, which corresponds to a value of the bulk crystal resistivity at 290 K. At 300 K, the resistivity values are the same as was already noted, (4-5)×10^{10} Ohm-cm. However, with an increase in the voltage, we observed a significantly

different dependence of the resistance on the voltage. Thus, in general, we can write that $\rho_{dif}=\rho_{dif}(U)$. For example, at ~500 V, the differential resistance of the In/Cd(Mn)Te/In structure decreases significantly and becomes ~ 2×10^8 Ohm-cm, while for the Ni/Cd(Mn)Te/In structure, the differential resistance increases to ~ 2×10^{12} Ohm-cm. The main mechanism that reduces the In/Cd(Mn)Te/In resistance is the currents, limited by the space charge (SCLC) [19,20]:

$$j_{SCLC}=\frac{9}{8}\Theta\varepsilon_s\mu_n\frac{U^2}{d^3}, \quad (2)$$

where Θ is the dimensionless parameter called the capture factor, μ_n is the electron mobility, d is the thickness of the crystal, $\varepsilon_s=\varepsilon_o\varepsilon$, ε_o is the electrical constant, and ε is the dielectric permittivity of the Cd(Mn)Te crystal. From the *I-V* characteristics of the In/Cd(Mn)Te/In structure, we can determine the product $\mu\cdot\tau$ [21]:

$$\mu_n\tau_n=d^2/U_{o1}, \quad (3)$$

where U_{o1} is the transition voltage to the SCLC, that is, to the quadratic dependence $I\sim U^2$ for In/Cd(Mn)Te/In, and τ_n is the lifetime. In our case, U_{o1} = 12 V (Fig. 1(a)) and according to (3) $\mu_n\tau_n=2\cdot10^{-3}$ cm^2 V^{-1}.

As for the *I-V* curve of the Ni/Cd(Mn)Te/In structure, the situation was somewhat more complicated. With an increase in voltage, the growth of dark current slowed down, and the *I-V* varies as the square root $I\sim U^{1/2}$. This *I-V* section is well described within the framework of the Sah-Noyce-Shockley theory in the case of Schottky-type Ni/Cd(Mn)Te contact. This was quite understandable, because, according to the generation theory in the SCR [22], when qV is much greater than kT, the factor [exp(qV/2kT)-1] does not manifest itself at high reverse voltages, and the dependence of I vs. U becomes $I\sim U^{1/2}$. Figs. 3(a, b) show a comparison of the fitting results based on the Sah-Noyce-Shockley model.

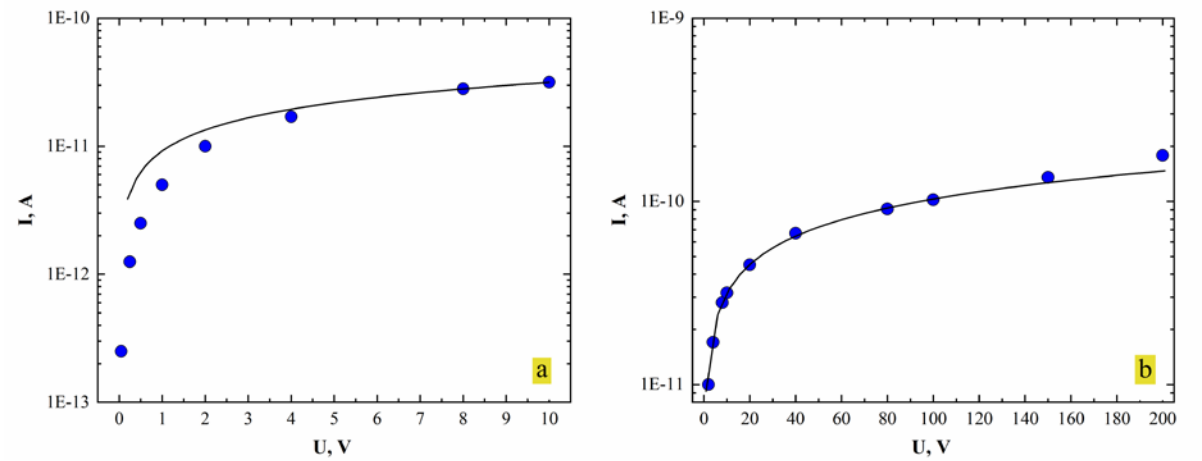

Fig. 3. Comparison of the experimentally measured (filled circles) and calculated (solid line) currents according to [18] and [22] for Ni/Cd(Mn)Te/In at reverse bias: (a) the initial section of the *I-VC*, and (b) at higher voltages. T = 290 K.

In calculations, the following parameters were used: the height of the Ni/Cd(Mn)Te potential barrier - φ_o = 0.75 eV, the energy position of the generation level - E_t = 0.83 eV, the concentration of non-compensated impurities - $N=10^{12}$ cm^{-3}, electron mobility - μ_n =700 cm^2/(V×s), hole mobility – μ_p = 70 cm^2/(Vs), an effective Shockley lifetimes for electrons and holes, respectively - $\tau_{no}=\tau_{po}=3\times10^{-8}$ s, and an effective masses of electrons and holes - $m_n=0.11m_o$, $m_p=0.65m_o$. As seen from Figs. 3 (a, b), a good agreement of the experiment and the calculations is observed in the range of 4-150 V. It is clear that up to 4 V, the curve is governed by Ohm's law, while above 150 V the SCLC effect dominates.

Indeed, with a further increase in the voltage, the sublinear *I-V* section gradually became linear $I\sim U$, followed by the quadratic $I\sim U^2$. That is, in form this section repeats the *I-VC* of the In/Cd(Mn)Te/In structure, only at significantly higher voltages. For the In/Cd(Mn)Te/In structure the voltage of the start of the quadratic dependence is U_{o1} ~ 12 V, and for the Ni/Cd(Mn)Te/In structure, the start of the quadratic section corresponds to the voltage of U_{o2} ~ 600 V. According to [18], the voltage at which the quadratic section becomes clearly seen is:

$U_{o2}=d^2/\mu_n\tau_{no}$, (4)

where τ_{no} is an effective Shockley lifetime [22]. Since, in our case $\tau_{no} << \tau_n$, according to (4), we can obtain a significantly higher voltage at the beginning of the *I-V* quadratic section for the Ni/Cd(Mn)Te/In structure. Knowing the U_{o2} value, we can evaluate the $\mu\tau$ values for both structures. However, for the Ni/Cd(Mn)Te/In structure, this product will be equal to $\mu_n\tau_{no} = 4\times10^{-5}$ cm^2 V^{-1}. For Ni/Cd(Mn)Te/In, $\mu_n\tau_{no}$ is substantially smaller than for that evaluated for the structure with ohmic contacts. This should be surprising, since in the strong electric field the Shockley's lifetimes τ_{no} operate, and not the equilibrium ones τ_n. Attention is also applied to this aspect in [23], where a somewhat more difficult method of product $\mu\cdot\tau$ estimation was used. It is worth noting that we also carried out measurements of $\mu\tau$ from the Hecht equation in the approximation for one type of charge carrier [24]:

$$CCE \approx \frac{\mu_n\tau_{no}E}{d}\left[1-\exp\left(\frac{-d}{\mu_n\tau_{no}E}\right)\right], \quad (5)$$

where E is the electric field strength. We obtained values close to the $\mu_n\tau_{no}=2\times10^{-5}$ cm^2 V^{-1}, which was also found from the *I-V*.

At higher voltages, there is a characteristic region $I\sim U^n$, where n=3.5 for both types of structures, but at different voltages. The transition voltage from the quadratic dependence to the power dependence is called the voltage of the traps' full filling U_{TFF} [19, 20]:

$$U_{TFF} = \frac{eN_t d^2}{3\varepsilon_S} \quad (6)$$

Using the value of U_{TFF}, the concentration of traps N_t can be determined. Voltage U_{TFF1} = 100 V for In/Cd(Mn)Te/In, and U_{TFF2} = 800 V for Ni/Cd(Mn)Te/In structures. The corresponding values N_t were found to be $N_{t1} = 7.4\times10^{10}$ cm^{-3} and $N_{t2} = 5.9\times10^{11}$ cm^{-3}. From the expression for U_o [20]:

$$U_0 = \frac{4d^2}{3\rho\ \mu_n\Theta\varepsilon_S}, \quad (7)$$

one can define Θ_1 and Θ_2 by substituting the corresponding values of U_{o1} and U_{o2} for the In/Cd(Mn)Te/In and Ni/Cd(Mn)Te/In structures, respectively. Finally, from (8) [20]:

$$\frac{N_c}{N_t}\cdot\exp\left[\frac{E_t-E_c}{kT}\right] = \Theta \quad , \quad (8)$$

it is possible to find the energy position of the trap levels E_{t1} and E_{t2}. After carrying out the necessary calculations, using (6-8), we found $\Theta_1 = 3\times10^{-7}$, $\Theta_2=3\times10^{-10}$ and E_{t1}=0.89-0.9 eV, E_{t2}= 0.78-0.8 eV, respectively.

The N_{t2} increases by almost an order of magnitude, which is due to the fact that in the case of the Ni/Cd(Mn)Te/In structure, a much greater voltage can be applied to the crystal and, accordingly, a much stronger electric field is possible in the crystal. This leads to a significant increase in the concentration of active levels, plus their energy positions are also changing.

We carried out measurements of the americium isotope emission spectra using the samples with the In/Cd(Mn)Te/In and Ni/Cd(Mn)Te/In structures. The results are shown in Fig. 4.

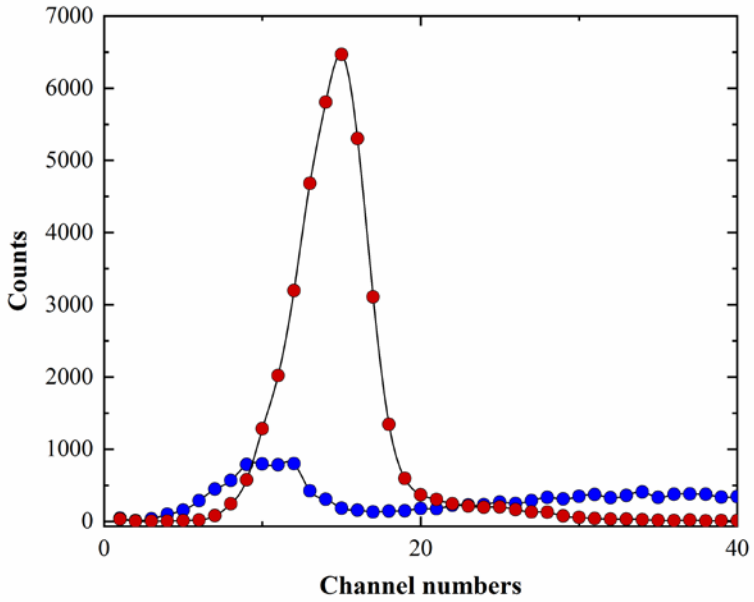

Fig. 4. Americium isotope emission spectra registered by the Ni/Cd(Mn)Te/In detector - red circles, voltage 350 V, “minus” to the nickel electrode, and In/Cd(Mn)Te/In - blue circles, voltage 250 V. T=300 K. FWHM is ~12.5 keV for Ni/Cd(Mn)Te/In.

As shown in Fig. 4, for the Ni/Cd(Mn)Te/In structure with rectifying contact, we observed a better sensitivity and better energy resolution. Significantly worse parameters for the In/Cd(Mn)Te/In structure with ohmic contacts could be attributed to the fact that the SCLC limits the maximum electric field strength possible for the crystal at a moderate dark current.

3. CONCLUSIONS

The n-Cd(Mn)Te structures with both ohmic and rectifying contacts were fabricated and tested. The bulk resistivity of the material was determined from the *I-V* ohmic section of the In/Cd(Mn)Te/In structure: 5×10^{10} Ohm-cm at 300 K. An analysis of the dark current mechanisms in structures with ohmic contacts and with a rectifying contact was carried out. For the structure with ohmic contacts, Ohm's law was observed in the beginning, and SCLC was seen at higher voltages. For the structure with a rectifying contact, the dark current has the generation character and SCLC at the high voltages. The In/Cd(Mn)Te/In structures with ohmic contacts were unsuitable for use as ionizing radiation detectors, because the dark currents quickly reached unacceptably large values at increased voltage. In spite of the fact that the $\mu_n\tau$ was found to be larger for the In/Cd(Mn)Te/In structure, the Ni/Cd(Mn)Ta structure allowed for a substantially higher electric field strength at moderate dark current. The measurements of the americium gamma-radiation spectrum by the Ni/Cd(Mn)Te/In and In/Cd(Mn)Te/In detectors fully confirmed these results.

REFERENCES

[1] Alan Owens, Compound Semiconductor Radiation Detectors. Series in Sensors. Taylor & Francis, October 26, 2016 by CRC Press.
[2] K. Zanio, and Fred H. Pollak, “Semiconductors and Semimetals”, Vol. 13 (Cadmium Telluride), Physics Today, 31(8), 53 (1978).
[3] R. Triboulet, P. Siffert, [CdTe and related compounds: physics, defects, technology, hetero- and nanostructures and applications: physics, CdTe-based nanostructures, and semi-magnetic semiconductors, defects], European Materials Research Society series. (Oxford: Elsevier, 2010).
[4] H. Shiraki, M. Funaki, Y. Ando, S. Kominami, K. Amemiya and R. Ohno, “Improvement of the productivity in the THM growth of CdTe single crystal as nuclear radiation detector”, IEEE Trans. Nucl. Sci. 57, 395 (2010).
[5] Tadayuki Takahashi, Shin Watanabe, Yuto Ichinohe, Hirokazu Odaka, Goro Sato, Shin’ichiro Takeda, “High Resolution CdTe detectors and Applications to Gamma-ray Imaging”, IEEE Nucl. Sci. Symposium, Valencia (2011).
[6] Acrorad Co. Ltd., https://www.acrorad.co.jp/index_en/products_en/cdte/cdte_products.html.

[7] P. Fochuk, Z. Zakharuk, Ye. Nykonyuk, I. Rarenko, M. Kolesnik, A. E. Bolotnikov, G. Yang, and R. B. James, "Advantages of a Special Post-Growth THM Program for the Reduction of Inclusions in CdTe Crystal", IEEE Trans. Nucl. Sci. 63(3), 1839 (2016).
[8] T.Terao, A.Koike, K.Takagi, H.Morii, T.Okunoyama and T.Aoki, "Characterization of CdTe diode detector with depletion layer modulation for energy discrimination X-ray imaging", 20th International Workshop on Radiation Imaging Detectors, Sundsvall, Sweden, Published by IOP Publishing for Sissa Medialab, JINST 14 C06017 (2019).
[9] K. H. Kim, S. H. Cho, J. H. Suh et al., "Gamma-Ray Response of Semi-Insulating CdMnTe Crystals", IEEE Trans. Nucl. Sci. 56(3), 858 (2009).
[10] Ji Jun Zhang, Lin Jun Wang, Jian Huang, Ke Tang, Zhen Wen Yuan, Yi Ben Xia, "Properties of CdMnTe Single Crystal Used in Nuclear Radiation Detectors", Advanced Materials and Processes: ADME, 311-313, 1209 (2011).
[11] R. Rafiei, D. Boardman, A. Sarbutt, D. A. Prokopovich, K. Kim, M. I. Reinhard, A. E. Bolotnikov, and R. B. James, "Investigation of the Charge Collection Efficiency of CdMnTe Radiation Detectors", IEEE Trans. Nucl. Sci. 59(3), 634 (2012).
[12] KiHyun Kim, G. S. Camarda, Anwar Hossain, J. Franc, Andrea Zappettini, A. E. Bolotnikov, Ryan Tappero, Yonggang Cui, Laura Marchini, "New Approaches for Making Large-Volume and Uniform CdZnTe and CdMnTe Detectors", IEEE Trans. Nucl. Sci. 59(4), 1510 (2012).
[13] R. Rafiei, M. I. Reinhard, K. Kim, D. A. Prokopovich, D. Boardman, A. Sarbutt, G. C. Watt, A. E. Bolotnikov, L. J. Bignell, and R. B. James, "High-Purity CdMnTe Radiation Detectors: A High-Resolution Spectroscopic Evaluation", IEEE Trans. Nucl. Sci. 60(2), 1450 (2013).
[14] Aaron L. Adams, Ezekiel O. Agbalagba, Julius O. Jow, John G. Mwathi, Alexander A. Egarievwe, Wing Chan, Matthew C. Dowdell, Utpal N. Roy, Stephen U. Egarievwe, "Thermal Annealing of CdMnTe Material Being Developed for Nuclear Radiation Detection Applications", IOSR-JMCE, 13(4), Ver. IV, 01-05 (2016).
[15] S.I. Budzulyak, D.V. Korbutyak, L.A. Demchyna, V.M. Yermakov, N.D. Vakhnyak, I.M. Rarenko, Z.I. Zakharuk, M.H. Kolisnyk, P.M. Fochuk, S.H. Dremlyuzhenko, I.Z. Misevych, "Method of growing of CdTe single crystals and their solid solutions $Cd_xZn_{1-x}Te$, $Cd_xMn_{1-x}Te$", (in ukr.), Patent of Ukraine for Utility Model No. 113185, 26.12.2016.
[16] L. A. Najam, N. Y. Jamil, R. M. Yousif, L. A. Najam, "Fabrication of CdMnTe semiconductor as radiation detector", Indian J. Phys. 86(4), 267 (2012).
[17] Ye. Nykoniuk, S. Solodin, Z. Zakharuk, S. Dremlyuzhenko, B. Rudyk, P. Fochuk, "Compensated donors in semi-insulating $Cd_{1-x}Mn_xTe$:In crystals", J. Cryst. Growth 500, 117 (2018).
[18] V. M. Sklyarchuk, V. A. Gnatyuk, W. Pecharapa, "Low leakage current Ni/CdZnTe/In diodes for X/γ-ray detectors", Nuclear Instr. and Methods in Physics Research, Section A 879, 101 (2018);
[19] M. Lampert and P. Mark, [Injection currents in Solids], (in rus.), Mir, Moscow, 416 (1973).
[20] Ye. A. Tutov, F. A. Tuma, V. I. Kukuev, "Mechanisms of current transfer in the Al/ZnO/Si structure", Condensed matter and interphase boundaries, (in rus.), 8(4), 334 (2006).
[21] V. M. Sklyarchuk, P. M. Fochuk, "Method for determination of charge transfer parameters in semi-insulating materials based on CdTe and its solid solutions", (in ukr.), Patent of Ukraine for Utility Model No. 87411, 10.02.2014.
[22] C. Sah, R. Noyce, W. Shockley, Proc. IRE, 45, 1228 (1957).
[23] A. E. Bolotnikov, G. S. Camarda, E. Chen, R. Gul, V. Dedic, G. De Geronimo, J. Fried, A. Hossain, J. M. MacKenzie, L. Ocampo, P. Sellin, S. Taherion, E. Vernon, G. Yang, U. El-Hanany, and R. B. James, "Use of the drift-time method to measure the electron lifetime in long-drift-length CdZnTe detectors", J. Appl. Phys. 120(10), 104507 (2016).
[24] Ruihua Nan, Wanqi Jie, Gangqiang Zha, Hui Yu, "Relationship between high resistivity and the deep level defects in CZT: In", J. Nucl. Instr. Meth. A 705, 32 (2013).